PERGAMON

International Journal of Multiphase Flow 26 (2000) 1–15

International Journal of Multiphase Flow

www.elsevier.com/locate/ijmulflow

Shear-induced particle resuspension in settling polydisperse concentrated suspension

Anat Shauly, Amir Wachs, Avinoam Nir*

Department of Chemical Engineering, Technion, Israel Institute of Technology, Haifa, 32000, Israel

Received 14 September 1998; received in revised form 13 December 1998

Abstract

A phenomenological model describing the resuspension of polydisperse suspension in shear flow is presented. The model combines mechanisms of hindered sedimentation and shear-induced particle migration. The latter is expressed in terms of migration potentials for mono and polydisperse mixtures. The calculated results agree well with available experimental observations. It predicts the rise and location of the suspension upper surface, the separation of species in the suspension and the location and sharpness of interfaces between species. It can be used to analyze the flow of concentrated polydisperse suspensions under gravity in complex geometries and to predict macroscopic properties associated with these flows. © 1999 Elsevier Science Ltd. All rights reserved.

1. Introduction

Heavy small particles that are settled in a lighter viscous fluid can resuspend if the mixture is exposed to a shear field. The shear induces a flux of particles, which can migrate in a direction opposite to that of gravity. When this flux and the sedimentation flux balance each other the particles remain resuspended. This phenomenon was first explained explicitly by Leighton and Acrivos (1986) who measured resuspension levels when a simple shear flow is forced over a settled layer of uniform spherical particles.

The resuspension phenomenon has direct important effect on the flow of suspensions. When the shear intensity is strong enough to induce the resuspension of entire amount of particles in the suspension a steady particle concentration distribution results, and a steady-state horizontal

* Corresponding author. Tel.: +972-4-829-2119; fax: +972-4-823-0476.

PII: S0301-9322(98)00086-X

or near horizontal flow of the suspension can be sustained. Nir and Acrivos (1990), Kapoor and Acrivos (1995) and Dahlkild (1997) studied the conditions needed for the existence of a steady slide of a layer of sediment on an inclined surface on which particles are settling at a constant rate. Schaflinger et al. (1990) and Zhang and Acrivos (1994) addressed the viscous resuspension in fully developed pressure driven laminar flows in two-dimensional and circular pipes, respectively.

There exist specific studies of the resuspension phenomenon which are distinguished by experiments in which the suspension was subject to a unidirectional shear flow with streamlines oriented perpendicular to the direction of gravity and with a well-defined velocity gradient. This facilitates the understanding of the effect of the interaction between gravity and shear-induced fluxes. These studies can be divided into two main categories according to whether the velocity gradient is parallel or perpendicular to gravity, which we shall henceforth term as the 'parallel case' and the 'perpendicular case', respectively. A schematic description is shown in Fig. 1. In the former case we note the works of Leighton and Acrivos (1986) and Chapman and Leighton (1991), who studied the resuspension of a monodisperse suspension of particles for which inertia effects and Brownian diffusion can be neglected. The simple shear field was obtained by the relative rotation of two parallel annular surfaces with the gap between them filled with the settled suspension. The results were expressed in terms of a dimensionless number, the Shields parameter, which denotes the ratio between shear and gravity forces on the particles. In such experiments the shear stress is constant across the gap of the annular device. Later, Krishnan and Leighton (1995) used a similar experimental setup to study the resuspension of bidisperse suspension and reported the effect found on the measured effective viscosity. No details on the resuspension of the individual species within the mixture were reported. In the perpendicular case the experimental apparatus used was a narrow gap concentric Couette flow device (Acrivos et al., 1993; Tripathi & Acrivos, 1998). In these works the shear rate across the cylindrical gap is constant. The principal measured result, i.e. the height of resuspension, was expressed in terms of a dimensionless parameter proportional to the constant shear rate. Acrivos et al. (1993) measured the resuspension of monodisperse suspensions while Tripathi and Acrivos (1998) studied bidisperse systems with one of the species being neutrally buoyant in the fluid.

The behavior of polydisperse systems is more complex than that observed in monodisperse suspensions. In neutrally buoyant suspensions undergoing shear, the intensity of shear-induced migration differs for different species and depends on particle size. This results in separation of species in the flow field (Graham et al., 1991; Krishnan et al., 1996; Shauly et al., 1998). In resuspension studies of polydisperse mixtures this phenomenon is further complicated by the existence of the gravity field, which induces additional separation of species due to size and density differences. In this communication we present a model which describes the resuspension and separation of polydisperse suspensions in a shear field. While Shauly et al. (1998) modeled and examined experimental studies of suspensions with freely suspended particles, this study involves migration under an external force field. The approach incorporates hindered settling and phenomenological shear-induced migration models and directly addresses the various experimental systems cited above. We calculate species concentration distributions, location and sharpness of interfaces, intensity of separation of species and total height of resuspension. Several interesting comparisons are made with the available experimental results.

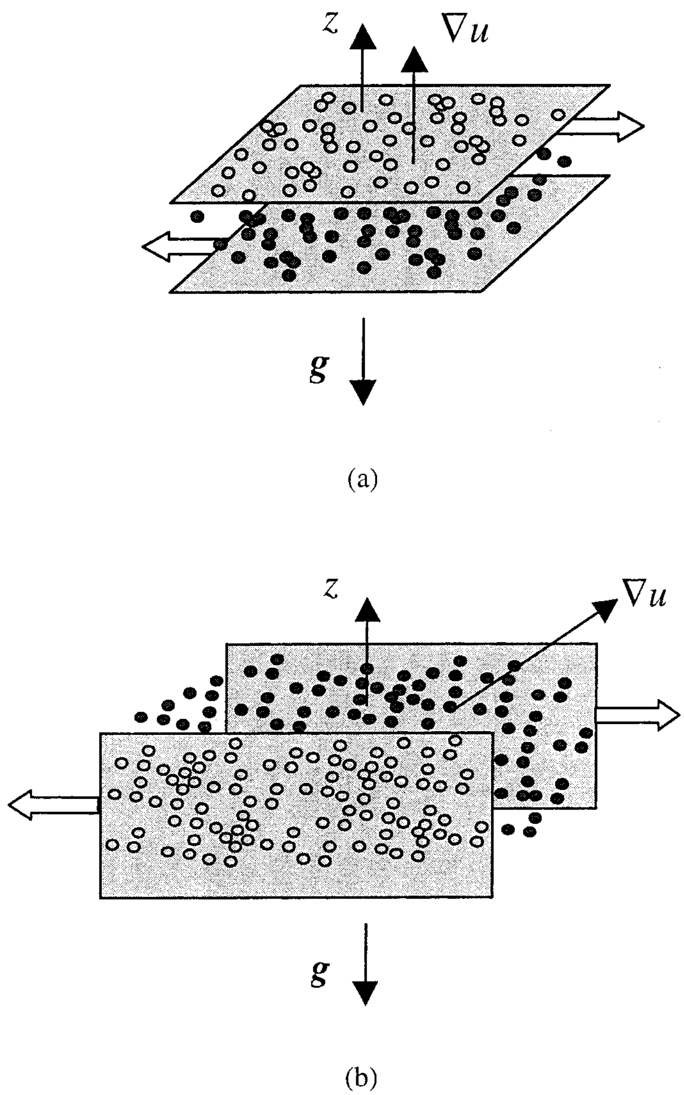

Fig. 1. Schematic description of resuspension experiments. (a) Parallel case with velocity gradient in the direction of gravity; (b) perpendicular case where the velocity gradient is normal to the direction of gravity.

2. A simple phenomenological model for resuspension

2.1. Monodisperse suspensions

The common approach to constructing a particle balance is to assume that the Stokesian particles are carried by the viscous fluid along the streamline on which they are located with the local fluid velocity. Let ϕ be the particle concentration and $\mathbf{u}$ be the macroscopic velocity field. The total change in particle concentration is

$$\frac{d\phi}{dt} = -\nabla \cdot \mathbf{J} \tag{1}$$

Here, the flux $\mathbf{J}$ is a combination of the sedimentation and the shear-induced fluxes which can carry particles across streamlines. For the sedimentation flux we adopt the form

$$\mathbf{J}_g = \mathbf{u}_t f(\phi)\phi \tag{2}$$

where $\mathbf{u}_t = 2\,\boldsymbol{g}(\rho - \rho_f)a^2/9\mu_f$ is the terminal settling velocity of a single particle in a very dilute suspension and $f(\phi)$ is the hindrance function. In Eq. (2) μ_f, ρ_f, a and ρ denote the fluid viscosity, fluid density, particle radius and particle density, respectively, and $\boldsymbol{g}$ is the acceleration of gravity. The shear-induced diffusion flux is expressed in terms of a particle migration potential $P = \ln(\phi\gamma\mu_s^{\lambda}\mathscr{R})$ (see Shauly et al., 1998) and has the form

$$\mathbf{J}_d = -\gamma a^2 \phi^2 \mathbf{K} \cdot \nabla P \tag{3}$$

Here, γ is the magnitude of the shear rate and $\mathbf{K}$ is a dimensionless coefficient for which we have given a tensorial form in anticipation that its values $k_{\|}$ and $k_{\perp}$ for the parallel and perpendicular cases, respectively, may differ. In the expression for the migration potential $\mu_s(\phi)$ denotes the effective viscosity of the suspension, $\mathscr{R}$ is the streamline curvature and λ is a constant. The form of the potential comprises all the known migration mechanisms as suggested by Leighton and Acrivos (1987), Phillips et al. (1992) and Krishnan et al. (1996). The values and forms of the various coefficients and effective properties are discussed further in this section and in the Appendix.

We conclude this formulation by considering the special case of a steady-state flow with streamlines of constant curvature and orthogonal to the direction of gravity and to the direction shear-induced flux. If no flux crosses the boundaries we have, everywhere,

$$\mathbf{J} = -\gamma a^2 \phi^2 \mathbf{K} \cdot \nabla \; \ln(\phi\gamma\mu^{\lambda}) + \mathbf{u}_t f(\phi)\phi = 0 \tag{4}$$

where $\mu = \mu_s/\mu_f$.

2.2. Polydisperse suspensions

Consider a polydisperse suspension containing several species of spherical particles with radius a_i and density ρ_i, and with local species concentration ϕ_i. The conservation equation for species i is of a form similar to that of Eq. (1) with the sedimentation flux being

$$\mathbf{J}_{gi} = \frac{2}{9}\frac{\boldsymbol{g}(\rho_i - \rho_f)a_i^2}{\mu_f} f_i \phi_i \tag{5}$$

where f_i is the hindrance function for species i and with the species shear-induced diffusion flux (Shauly et al., 1998)

$$\mathbf{J}_{di} = -\gamma \bar{a} a_i \phi \phi_i \mathbf{K} \cdot \left[\nabla \; \ln(\phi_i \gamma \mu^{\lambda} \mathscr{R}) - \left(1 - \frac{\bar{a}}{a_i}\right) \nabla \; \ln \; \mu^{\lambda} - \left(1 - \frac{a_i^q}{\bar{a}^q}\right) \nabla \; \ln \; \mathscr{R} \right] \tag{6}$$

Here

$$\phi = \sum_i \phi_i \text{ and } \overline{a^n} = \frac{\sum_i a_i^n \phi_i}{\phi} \tag{7}$$

and q is a constant. In Eq. (6) the effect of polydispersivity is explicitly encountered in the last two terms. The interactions of a particle with the effective viscosity gradient and with the gradient of the streamline curvature depend on the particle relative size and, as is shown in Shauly et al. (1998), the corresponding effect on the migration of species of different particle size is opposite. Under the conditions leading to Eq. (4) we have, for the polydisperse case, the simplified species balance

$$\mathbf{J}_i = -\gamma \bar{a} a_i \phi \phi_i \mathbf{K} \cdot \left[\nabla \ \ln \ (\phi_i \gamma) + \frac{\bar{a}}{a_i} \nabla \ \ln \ \mu^{\lambda} \right] + \frac{2}{9} \frac{\mathbf{g}(\rho_i - \rho_{\mathrm{f}}) a_i^2}{\mu_{\mathrm{f}}} f_i \phi_i = 0 \tag{8}$$

This equation reduces to Eq. (4) when the suspension is monodisperse. We shall use these balances in the following section to analyze various experimental studies with parallel and perpendicular cases.

2.3. Coefficients and effective properties

When applying Eqs. (4) and (8) in particular cases one must introduce explicit forms to the effective properties μ, f and f_i. In this paper we used, for the monodisperse systems, the expression for the effective viscosity suggested by Leighton and Acrivos (1986)

$$\mu = \frac{\mu_{\mathrm{s}}}{\mu_{\mathrm{f}}} = \left(1 + \frac{1.5\phi_m \phi}{\phi_m - \phi} \right)^2 \text{ with } \phi_m = \phi_{m0} = 0.58 \tag{9}$$

and for the hindrance function the approximation $f(\phi) = (1 - \phi)/\mu$. For the polydisperse suspensions the dependence of μ on the various ϕ_i and a_i is embedded in ϕ_m via an empirical expression $\phi_m = \phi_m(\phi_{m0}, a_i, \bar{a}, \phi_i, \phi)$ as described in the Appendix (see also Shauly et al., 1998, for details). For the hindrance effect the product $(\rho_i - \rho_f) f_i / \mu_{\mathrm{f}}$ in Eq. (5) is expressed as $(\rho_i - \rho_{\mathrm{s}})/\mu_{\mathrm{s}}$ with $\rho_{\mathrm{s}} = \rho_{\mathrm{f}}(1 - \phi) + \Sigma \rho_j \phi_j$ being the suspension effective density.

The values of the coefficients λ and $\mathbf{K}$ are estimated independently from available data obtained in steady and transient state experiments with shear-induced migration in the absence of gravity. From the data of Phillips et al. (1992) Shauly et al. (1998) obtained the estimate $\lambda \approx 2$. The same data also suggests that $k_{\parallel} \approx 0.4$ for the parallel case. No independent estimate was found for $k_{\perp}$.

2.4. Further simplified equations

We conclude this section by obtaining simple sets of equations for the particular parallel and perpendicular cases. In the former case the mixture is sheared between two surfaces, separated by a distance $2b$, with the gravity and velocity gradients parallel to each other. We let the coordinate in this direction be denoted by z and render all variables dimensionless using b, μ_f and the values of a and $\Delta\rho = \rho - \rho_f$ associated with a typical particle. The sum of all $\mathbf{J}_i = 0$ in Eq. (8) yields

$$\frac{d}{dz}\ln(\bar{a}\phi\mu^{\lambda-1}) = -\frac{2}{9k_{\parallel}\phi\Psi}\left\{\sum_i\left[\left(\frac{a_i}{a}\right)^2\frac{\phi_i}{\phi}\Delta\rho_i\right] - \frac{\overline{a^2}}{\bar{a}^2}\sum_i[\Delta\rho_i\phi_i]\right\} \tag{10}$$

while the difference between any two species fluxes, say $\mathbf{J}_i - \mathbf{J}_j$, obtains the form

$$\frac{d}{dz}\ln\left(\frac{\phi_i^{a_i}}{\phi_j^{a_j}}\mu^{a_j-a_i}\right) = -\frac{2}{9k_{\parallel}\bar{a}\phi\Psi}\{(a_i^2\Delta\rho_i - a_j^2\Delta\rho_j) - (a_i^2 - a_j^2)\sum_k[\Delta\rho_k\phi_k]\} \tag{11}$$

In Eqs. (10) and (11) Ψ is a modified Shields parameter with b replacing the particle size, $\Psi = \tau/(gb\Delta\rho)$, τ denotes the constant shear stress magnitude across the gap and $g = |\boldsymbol{g}|$. $\Delta\rho_i$ stands for the difference $\rho_i - \rho_f$.

In the perpendicular case the chosen length scale is the initial height of the settled sediment, h_0. The experiments were typically carried out in a narrow gap concentric Couette cell so that the shear rate was constant along the axis of the device. The set of equations, obtained by taking the sum and differences as above, is similar and has the dimensionless form

$$\frac{d}{dz}\ln(\bar{a}\phi\mu^{\lambda}) = -\frac{1}{k_{\perp}\mu\phi A}\left\{\sum_i\left[\left(\frac{a_i}{\bar{a}}\right)^2\frac{\phi_i}{\phi}\Delta\rho_i\right] - \frac{\overline{a^2}}{\bar{a}^2}\sum_i[\Delta\rho_i\phi_i]\right\} \tag{12}$$

and

$$\frac{d}{dz}\ln\left(\frac{\phi_i^{a_i}}{\phi_j^{a_j}}\right) = -\frac{1}{k_{\perp}\bar{a}\mu\phi A}\{(a_i^2\Delta\rho_i - a_j^2\Delta\rho_j) - (a_i^2 - a_j^2)\sum_k[\Delta\rho_k\phi_k]\} \tag{13}$$

Here the dimensionless parameter is $A = (9\mu_f\gamma)/(2\ \ h_0 g\Delta\rho)$.

We shall use Eqs. (10)–(13) to calculate results relevant to various experiments. It is worth noting at this stage that a common characteristic can be obtained by examining the asymptotic behavior of any of the two sets. There can be only one interface where any species concentration becomes zero and this is the location where all species concentrations vanish. This is readily explained by the shear-induced diffusion mechanisms. A species' ability to diffuse depends on the concentrations of all other species and thus any ϕ_i, small as it can be, cannot become identically zero at a location where the total concentration ϕ is not zero.

3. Application to analysis of experimental studies

In this section we shall use the phenomenological model developed above to examine several selected experimental results, which have been reported in the literature so far. The purpose of this examination is to demonstrate that the model captures the behavior of the observed systems and that it can be further utilized to illuminate macroscopic properties or to predict microscopic local variables that were not or are too difficult to measure in polydisperse systems. The comparison is also useful to assess the extent of validity of various assumptions made in these experimental studies.

3.1. Parallel cases

The leading work of Leighton and Acrivos (1986) reported the rise of the interface of a settled layer of particles due to resuspension when sheared between parallel surfaces. Leighton and Acrivos show results of five different monodisperse systems with various suspension properties. In all runs it was evident that the elevated interface level varied linearly with Ψ. The measured slopes were 1.96, 2.1, 2.2, 2.2 and 3.3 (the last odd result was attributed to the presence of density polydispersivity). Our model prediction for this slope, using Eq. (1), is 2.35. Leighton and Acrivos' (1986) evaluation, based on a slightly different diffusion model, yielded 1.9. Hence, both calculations agree with the experimental observations.

Chapman and Leighton (1991) used a similar geometry to study the dynamical behavior of monodisperse suspensions when subject to a step in the imposed shear. To facilitate a quantitative description of the measured results they assumed that the particle concentration profile in the sheared suspension is linear along the gap between the shearing surfaces. Using this assumption they obtained a linearization of the highly non-linear Eq. (1) and an approximate solution. From this solution Chapman and Leighton (1991) obtained the dynamic change of the effective viscosity, presumably deduced from the imposed torque, and the mean square of the difference between the local and the average suspension concentration across the gap, $\langle(\Delta\phi)^2\rangle$, as a function of Ψ.

In order to make a comparison between these results and the present model we calculated concentration profiles across the gap for various values of Ψ. These are depicted in Fig. 2. It is

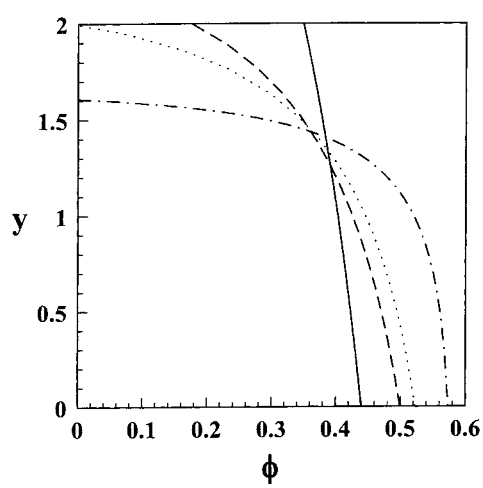

Fig. 2. Particle concentration profiles for resuspension in a parallel case calculated for a monodisperse suspension with average concentration $\phi_s = 0.4$. The solid, dashed, dotted and dash–dotted curves correspond to $1/\Psi^2$ values of 0.5, 5, 10 and 100, respectively.

clear that the three profiles, which correspond to cases in the range of data of Chapman and Leighton (1991) at Ψ^2 values of 0.01, 0.1 and 0.2, are far from being linear. We anticipate that such nonlinear profiles are expected irrespective of the choice of shear-induced diffusion model, and that the linear concentration profile assumption would apply only at very high values of Ψ beyond those measured. A consequence of this assumption at every Ψ is that it can lead to large overestimates of the values of $\langle(\Delta\phi)^2\rangle$ and the observed effective viscosity (cf. Eq. (6) in Chapman and Leighton, 1991). Fig. 3 shows the dependence of $\langle(\Delta\phi)^2\rangle$ on $1/\Psi^2$. The solid curve is the result of our calculations using an integration of Eq. (10). The squares and circles are estimates calculated by Chapman and Leighton (1991) by fitting the linearized model to their experiments. Note that the vertical dashed line at $\Psi^2 \approx 0.1$ separates two regions. At higher values of Ψ the particles are resuspended throughout the entire gap while when $\Psi^2 < 0.1$ the content of the gap consists of two layers with a clear fluid layer flowing on top of a resuspended suspension. Our calculation agrees well with the measurements of Chapman and Leighton (1991) in predicting the location of this division.

A parallel case study of the resuspension of bidisperse systems was reported by Krishnan and Leighton (1995). The same shear geometry as in the studies above was used. They have also extended the model of Chapman and Leighton (1991) to analyze the dynamic response of the effective viscosity of the bidisperse suspension to step increase of the imposed shear rate. This extended model now rests on two major assumptions: the concentration profile is linear and the two particle species remain well mixed. We have used Eqs. (10) and (11) to calculate concentration profiles in a sheared bidisperse suspension with the choice of parameters taken from the data of Krishnan and Leighton (1995). These are shown in Fig. 4. Evidently, the calculated profiles of the total concentration in these cases are not linear. This is similar to the result obtained for the monodisperse system. Furthermore, there is a considerable separation of

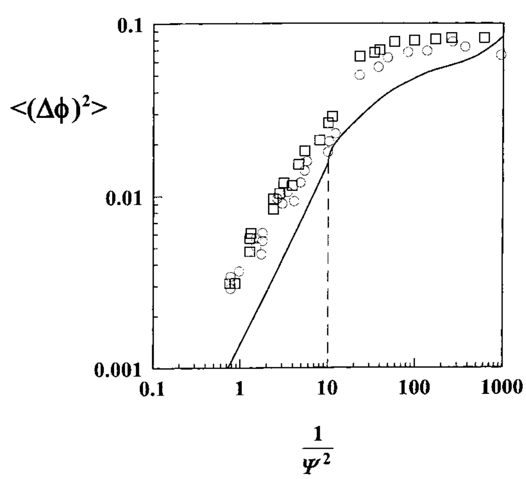

Fig. 3. Mean square concentration deviation versus Ψ for resuspension in a monodisperse parallel case. The average suspension concentration is $\phi_s = 0.4$. The squares and circles are calculation by Chapman and Leighton (1991) using linear profile approximation. The solid line is the prediction of this model. The region to the right of the dashed vertical line near $\Psi^2 = 0.1$ is where there exists a clear fluid layer above the resuspended suspension.

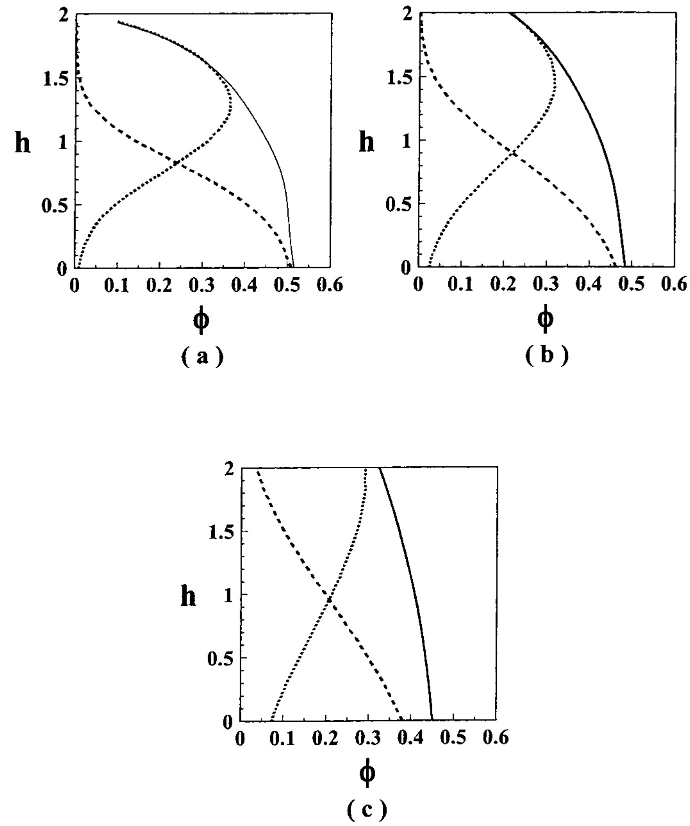

Fig. 4. Total and species concentration profiles for resuspension in a parallel case calculated for a bidisperse suspension with equal amounts of large and small spheres and with an average particle concentration $\phi_s = 0.4$. The solid curve shows the total concentration and the dashed and dotted profiles correspond to concentrations of species with densities, relative to that of the fluid, 2.034 and 1.966, and with size ratio $a_1/a_2 = 2.357$ (as in Krishnan and Leighton, 1995). (a)–(c) correspond to $1/\Psi^2$ values of 10, 4 and 1, respectively.

sizes, which is evident even at $\Psi = 1$. Thus, an effective viscosity can only be defined locally and not for the entire suspension since the composition of the bidisperse mixture changes rather dramatically with position. There may be two causes for the observed separation of species in the experiments of Krishnan and Leighton (1995). There are different particle sizes ($a_1/a_2 = 2.357$) and a slight different particle density in each of the species ($\Delta\rho_1/\Delta\rho_2 = 1.07$). Note that, in this flow field, the streamline pattern has a uniform zero curvature. To investigate this further we have calculated the particle concentration distributions with $\Delta\rho_1 = \Delta\rho_2$. The profiles obtained are almost identical to those depicted in Fig. 4. We have also calculated these profiles for the same size ratio but with the density difference ratio reversed (i.e. with $\Delta\rho_2/\Delta\rho_1 = 1.07$). The resulting distribution shows, again, a considerable separation of the species with the *smaller* and *heavier* particles suspended on top of the others. Thus, we conclude from these runs that the dominant contributor to the species separation, with this set of physical parameters, is the size difference which affects the shear-induced migration mechanism via the

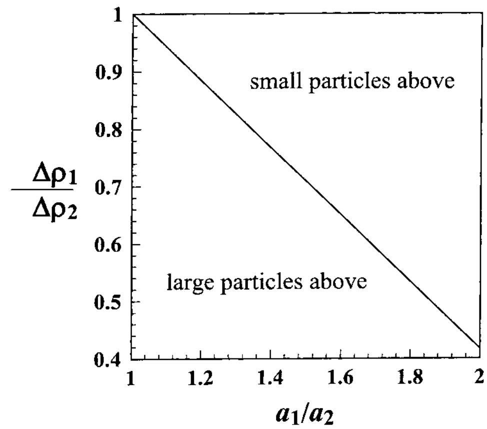

Fig. 5. Phase plane describing the separation regions of species in resuspension of a bidisperse mixture in a parallel case. The transition line is located, approximately, where the concentration profiles of the two species are similar along the entire gap.

non-uniform effective viscosity distribution along the resuspended layer, and directly affects the species sedimentation rate. It is interesting to explore the conditions at which the separation is reversed, i.e. the *lighter* and *larger* particles become suspended above the *heavier* and *smaller* particles. Fig. 5 shows such transition curve for various size and density difference ratios. Note that this transition is by no means sharp since the concentration profiles of the two species coincide only at equal size and density difference. Indeed, as a_1/a_2 increases along this transition line, a layer richer in the *larger* and *lighter* particles develops at an intermediate height sandwiched between two layers which are richer in the smaller heavy particles. This phenomenon is depicted in Fig. 6 and, evidently, calls for experimental corroboration.

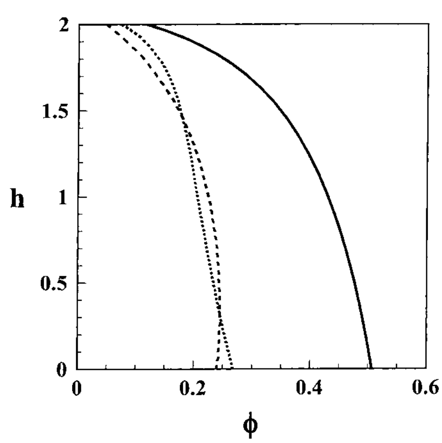

Fig. 6. Concentration distributions as in Fig. 4 with $a_1/a_2=2$, $\Delta\rho_1/\Delta\rho_2=0.4167$ and $1/\Psi^2=4$. Note the intermediate sub-layer, richer in species 1, which develops in the resuspended layer.

3.2. Perpendicular cases

The resuspension of a monodisperse suspension in a concentric narrow gap Couette cell was studied by Acrivos et al. (1993). The rise of the interface relative to the initial height of the sediment layer, $h = 1$, was reported as a function of the dimensionless parameter A defined in Section 2. Fig. 7 shows the data of Acrivos et al. (1993) together with a calculated curve using Eq. (12). Unfortunately, there are no other dynamic data from which $k_\perp$ could be estimated independently. We have used in this calculation $k_\perp = 0.12$ which is about one-third of the estimate of $k_\parallel$. Thus, the model and the data for the monodisperse parallel and perpendicular cases support the suggestion that the shear-induced diffusivity is, indeed, anisotropic. We have further used these findings to analyze perpendicular experiments with polydisperse suspensions.

Recently, Tripathi and Acrivos (1998) studied the resuspension of a bidisperse mixture in a narrow gap Couette device. They recorded the rise of the interface depending on particle concentration and the parameter A. The experimental system used had one species heavier than the fluid and the other species, which was rendered transparent, was neutrally buoyant. All particles were of the same size. Tripathi and Acrivos (1998) measured the location of the interface, arbitrarily defined as the height where the concentration of the heavy particles is 0.02. They also reported qualitative observations on the sharpness of the observed interface. We have used Eqs. (12) and (13) to simulate their experiments. In Fig. 8 we show profiles, of the total concentration and of the two species, as a function of the height along the cylinder's axis. Note that, at relatively low values of the parameter A and the concentration of the neutrally buoyant species, the interface appears very sharp. As the values of these parameters increase the two species further interpenetrate and the interface becomes fuzzy. These agree with the qualitative experimental observations. Note also that, although the concentration of the heavy particles become extremely small above the interface and far from the suspension upper surface, it never actually obtains the value zero anywhere in the bulk. This was also

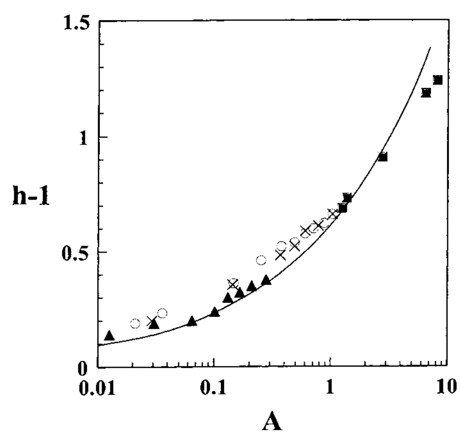

Fig. 7. The relative height of the resuspended layer of a monodisperse suspension in a perpendicular case as a function of the parameter A. The symbols depict data taken from Acrivos et al. (1993). The solid line is a result of this model.

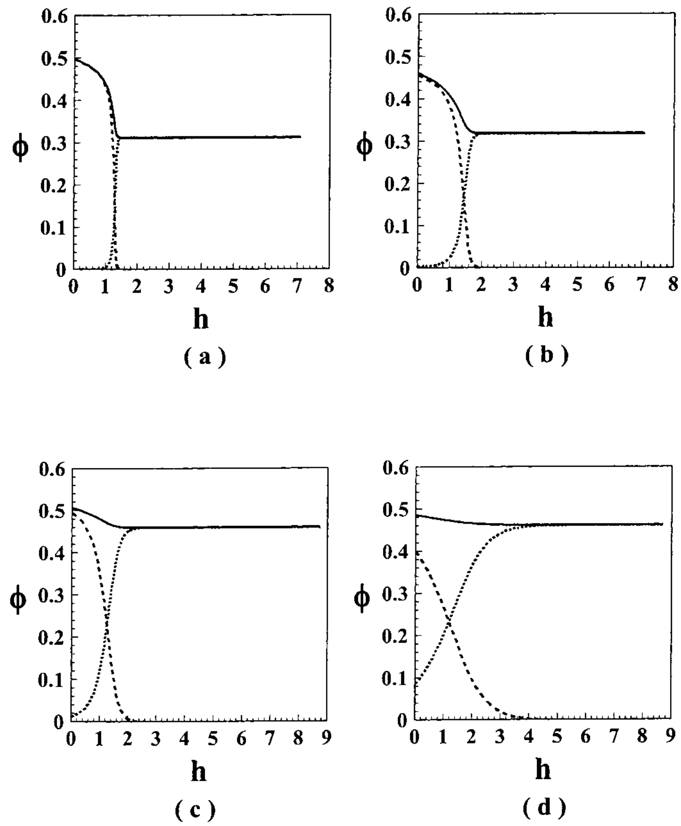

Fig. 8. Total and species concentration profiles for resuspension in a perpendicular case calculated for a bidisperse suspension with spheres of equal size for various values of the parameters A and $\phi*$. The solid curve shows the total concentration and the dashed and dotted profiles correspond to concentrations of species with densities relative to that of the fluid, 1.115 and 1.0, respectively (as in Tripathi and Acrivos, 1998). $\phi*$ denotes the concentration of the neutrally buoyant species in the fluid above a settled heavier layer of height $h = 1$ before the application of shear. (a) $A = 0.17$, $\phi* = 0.3$; (b) $A = 0.51$, $\phi* = 0.3$; (c) $A = 0.17$, $\phi* = 0.45$; (d) $A = 0.51$, $\phi* = 0.45$.

evident in the experiments where heavy particles could be occasionally observed near the upper surface. A quantitative comparison of the location of the measured interface and the one calculated using Eqs. (12) and (13) is shown in Fig. 9 where we have used the value $k_{\perp} = 0.12$ as estimated from the data in the monodisperse suspension case. The data and the calculations, which are completely independent, agree very well.

Acknowledgements

This work was supported by grant no. 92-00071 from the US–Israel Bi-national Science Foundation (BSF), Jerusalem, Israel. One of the authors, A. Nir, gratefully acknowledges the

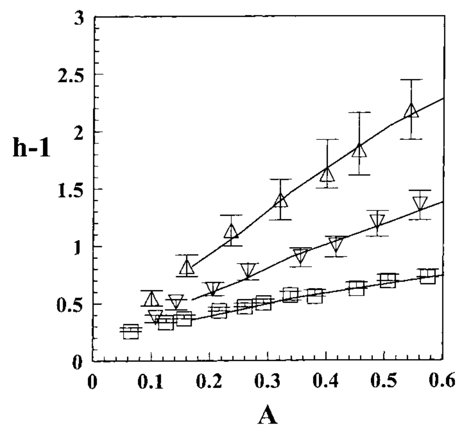

Fig. 9. The relative height of the resuspended layer of a bidisperse suspension in a perpendicular case as a function of the parameter A. The data is taken from Tripathi and Acrivos (1998). The solid lines are predictions of this model. $\phi*$ and the densities are as in Fig. 6. (□), (▽) and (△) correspond to $\phi*$ values of 0.3, 0.4 and 0.45, respectively.

hospitalities of the Advanced Mineral and Particle Center at the University of Melbourne and of the University of California at Santa Barbara during a sabbatical stay.

Appendix A

Revay and Higdon (1992) simulated the hindered settling of a suspension of equal-sized spheres. Computing mobility matrices they suggested the following expression for the hindrance function:

$$f(\phi) = (1-\phi)^{6.55}(1+3.458\phi^2+8.990\phi^3) \tag{A1}$$

For polydisperse suspensions with various particle sizes such an expression is not yet available and the common approach is to use the approximation

$$f(\phi) = (1-\phi)/\mu \tag{A2}$$

with μ being the effective viscosity. In Fig. A1 we show a comparison of $f(\phi)$, calculated from Eq. (A1), with two empirical expressions of the type Eq. (A2) which incorporate expressions for μ for monodisperse suspensions suggested by Krieger (1972), $\mu=(1-\phi/\phi_m)^{-1.82}$ with $\phi_m=0.68$ and by Leighton and Acrivos (1986) (see Eq. (9)). In the region where the shear-induced migration effect is significant, i.e. at $\phi > 0.2$, the latter expression follows the rigorous calculation much closer. We therefore used the expression of Leighton and Acrivos (1986) in the calculations performed throughout this paper.

For polydisperse suspensions one must account for the dependence of the effective viscosity on the concentrations and sizes of the various species. This can be accomplished through the value of ϕ_m. We followed here Shauly et al. (1998) who used an empirical expression for ϕ_m suitable for use with bidisperse suspensions which agrees well with various experimental results

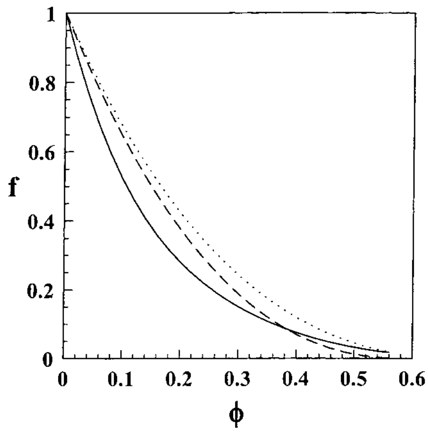

Fig. A1. A comparison between the hindrance function calculated after Revay and Higdon (1992) using Eq. (A1) (solid curve) and expressions of the form Eq. (A2). The dashed and dotted curves were calculated using expressions for μ suggested by Leighton and Acrivos (1986) and Krieger (1972), respectively.

and other empirical estimates, and in which the maximum concentration is corrected by

$$\frac{\phi_m}{\phi_{m0}} = \left[1 + \frac{3}{2} \mid b \mid^{\frac{3}{2}} \left(\frac{\phi_1}{\phi}\right)^{\frac{3}{2}} \left(\frac{\phi_2}{\phi}\right)\right] \text{ with } b = \frac{a_1 - a_2}{a_1 + a_2} \tag{A3}$$

References

Acrivos, A., Mauri, R., Fan, X., 1993. Shear-induced resuspension in a Couette device. Int. J. Multiphase Flow 19, 797–802.

Chapman, B.K., Leighton, D.T., 1991. Dynamic viscous resuspension. Int. J. Multiphase Flow 17, 469–483.

Dahlkild, A.A., 1997. The motion of Brownian particles and sediment on an inclined plate. J. Fluid Mech. 337, 25–47.

Graham, A.L., Altobelli, S.A., Fukushima, E., Mondy, L.A., Stephens, T.S., 1991. Note: NMR imaging of shear-induced diffusion and structure in concentrated suspensions undergoing Couette flow. J. Rheol. 35 (1), 191–201.

Kapoor, B., Acrivos, A., 1995. Sedimentation and sediment flow in settling tanks with inclined walls. J. Fluid Mech. 290, 39–66.

Krieger, I.M., 1972. Rheology of monodisperse lattices. Adv. Colloid Interface Sci. 3, 111–136.

Krishnan, G.P., Leighton, D.T., 1995. Dynamic viscous resuspension of bidisperse suspensions—I. Effective diffusivity. Int. J. Multiphase Flow 21, 721–732.

Krishnan, G.P., Beimfohr, S., Leighton, D.T., 1996. Shear-induced radial segregation in bidisperse suspensions. J. Fluid Mech. 321, 371–393.

Leighton, D., Acrivos, A., 1986. Viscous resuspension. Chem. Engng Sci. 41, 1377–1384.

Leighton, D., Acrivos, A., 1987. The shear-induced migration of particles in concentrated suspensions. J. Fluid Mech. 181, 415–439.

Nir, A., Acrivos, A., 1990. Sedimentation and sediment flow on inclined surfaces. J. Fluid Mech. 212, 139–153.

Phillips, R.J., Armstrong, R.C., Brown, R.A., Graham, A.L., Abbot, J.R., 1992. A constitutive equation for concentrated suspensions that accounts for shear-induced particle migration. Phys. Fluids A 4, 30–40.

Revay, J.M., Higdon, J.J.L., 1992. Numerical simulation of polydisperse sedimentation: equal-sized spheres. J. Fluid Mech. 243, 15–32.

Schaflinger, U., Acrivos, A., Zhang, K., 1990. Viscous resuspension of a sediment within a laminar and stratified flow. Int. J. Multiphase Flow 16, 567–578.

Shauly, A., Wachs, A., Nir, A., 1998. Shear-induced particle migration in a polydisperse concentration suspension, J. Rheol. (in press).

Tripathi, A., Acrivos, A., 1998. Viscous resuspension in a bidensity suspension, Int. J. Multiphase Flow 25, 1–14.

Zhang, K., Acrivos, A., 1994. Viscous resuspension in fully developed laminar pipe flows. Int. J. Multiphase Flow 20, 579–591.